Preparation and Characterization of Nanocrystalline Cellulose using Ultrasonication Combined with a Microwave-assisted Pretreatment Process

Zaira Z. Chowdhury* and Sharifah Bee Abd Hamid

This study focuses on the extraction of nanocrystalline cellulose (NCC) from the dried stalk of *Corchorus olitorius*, commonly known as jute, using a combination of a microwave-assisted alkaline peroxide pulping process (AHP) and ultrasonication. Dried jute stalk powder was pretreated using sodium hydroxide under microwave irradiation for the removal of lignin. The partially delignified sample was bleached using 30% hydrogen peroxide solution. The resulting crude cellulose was hydrolyzed using ultrasonication in the presence of ionic liquid and sulfuric acid. The effect of hydrolyzing medium on the physicochemical characteristics of the extracted nanocellulose was investigated. The nanocrystalline cellulose (NCC) obtained after combined treatments was rod-like, with diameters of 10 to 15 nm and lengths of 92 to 105 nm. Fourier transform infrared spectroscopy (FTIR) and X-ray diffraction analysis (XRD) showed that some breakages of intramolecular hydrogen bonds and glycosidic bonds occurred during the hydrolysis reaction of pretreated biomass. Ultrasonication in the presence of an acid hydrolyzing medium most effectively accelerated these breakages in the long chain cellulose biopolymer, leading to the formation of nanocrystalline cellulose (NCC) with higher crystallinity.

Keywords: Biomass; Nanocrystalline Cellulose (NCC); Ultrasonication; Hydrolysis; Alkaline peroxide pulping process (AHP)

Contact information: Nanotechnology and Catalysis Research Center (NANOCAT), University Malaya, Kuala Lumpur 50603, Malaysia;
** Corresponding author: zaira.chowdhury76@gmail.com, dr.zaira.chowdhury@um.edu.my*

INTRODUCTION

The delignification of renewable biomass for the extraction of advanced materials such as micro- and nanodimensional cellulose has become an attractive arena of research (Kalia *et al.* 2014). Biomass substrate can provide cellulosic materials with distinctive physico-chemical properties with little impact on the environment (Wicklein and Salazar-Alvarez 2013; Xu *et al.* 2013; Hossain *et al.* 2014; Kengkhetkit and Amornsakchai 2014). Cellulose is the most abundantly available biopolymer and is primarily found in plant biomass, but it can also be obtained from some animals (*e.g.*, tunicates), algae, and a few bacteria (Henriksson and Berglund 2007; Iwamoto *et al.* 2007). It is a kind of semi-crystalline polysaccharide consisting of β-D-glucopyranose units connected by β-1,4 glycosidic linkages (Chowdhury *et al.* 2014). Micro- (MCC) and nanocrystalline cellulose (NCC) usually exhibit unique properties, such as large surface area, high elastic modulus, high aspect ratio, and non-abrasive, non-toxic features with less thermal expansion. They are widely used as reinforcing agents in polymer nanocomposites (Klemm *et al.* 2011; Moon *et al.* 2011; Jiang *et al.* 2013a,b;

Abdul Khalil *et al.* 2014). NCC is used to fabricate optically transparent films with excellent visible light transmittance (Fukuzumi *et al.* 2013). The versatile properties of nanofibrillated cellulose allow it to be used in medicine, tissue engineering scaffolds, catalysis, textiles, surface coatings, drug delivery, and food packaging (Deng *et al.* 2010; Das *et al.* 2011; Klemm *et al.* 2011; Sacui *et al.* 2014).

The existence of hemicellulose and lignin in biomass substrate is intended to impart strength to the cell walls of plant residues and shield cellulose from chemical disintegration. Thus, the efficient pretreatment of lignocellulosic biomass must be addressed for delignification as well as the release of cellulosic content for ultimate transformation into nanocrystalline cellulose (NCC). The supra-molecular chain of cellulose contains a disordered amorphous domain, which is preferentially hydrolyzed by chemical treatment. However, the crystalline region of cellulose is rather more difficult to attack, as it is bonded by strong and complicated intra- and intermolecular hydrogen bonding. The extraction of cellulose from the lignocellulosic matrix and its digestion into nano-fibrillated cellulose is encumbered by numerous physiochemical, structural, and compositional aspects. Nanocellulose can be isolated by mechanical treatments, such as high-pressure homogenization (Nakagaito and Yano 2004; Stenstad *et al.* 2008), ultrasonication (Chen *et al.* 2011), cryocrushing (Chakraborty *et al.* 2005), microfluidization (Ferrer *et al.* 2012), and by chemical treatments such as TEMPO-mediated oxidation and acid and enzymatic hydrolysis (Sacui *et al.* 2014). Until recently, nano-structured cellulose has been synthesized from various types of biomass residue, such as rice straw (Jiang and Hsieh 2013b), mulberry barks (Li *et al.* 2009), sugarcane bagasse (Li *et al*. 2012), agricultural residues (Uma Maheswari *et al.* 2012), corncob (Silvério *et al.* 2013), cotton linters (Morais *et al.* 2013), mengkuang leaves (Sheltami *et al.* 2012), bamboo (Nguyen *et al.* 2013), and hemp and flax fiber (Mondragon *et al.* 2014).

Currently, pretreatment methods using microwave heating have gained attention. Basically, microwave irradiation can generate volumetric heating within a short timespan by initiating efficient internal heating through a combination of microwave energy with reactant molecules present in the reaction mixture (Kappe 2009). This provides rapid energy-efficient heating of the biomass substrate and can yield NCC within a short period of reaction time. Microwave-assisted acid hydrolysis was used to extract NCC from microcrystalline cellulose (MCC) (Kos *et al.* 2014).The extraction process was very fast. Within 10 min, 38% NCC was extracted using 60% sulfuric acid at 70 ^{o}C temperature (Kos *et al.* 2013). Compared with microwave heating, conventional heating is relatively slow and inefficient (Yin 2012). It has been previously reported that microwave irradiation can increase organic reaction efficiency, have a severe impact on the ultrastructure of cellulose, and degrade the lignin and hemicellulose of biomass (Zhang and Zhao 2010; Binod *et al.* 2012). However, to improve NCC yield and dispersion, acid hydrolysis has been widely used (Lai and Idris 2013). Acid hydrolysis aids in the breaking of the disordered and amorphous region of cellulose, which eventually releases single and well-defined nano-fibrillated cellulose. The acid hydrolysis process has been extensively used to prepare nanocellulose from wood (Revol *et al.* 1992), sisal (Moran *et al.* 2008), bacterial cellulose (Araki and Kuga 2001; Roman and Winter 2004), wheat straw (Helbert *et al.* 1996), and tunicate cellulose (Favier *et al.* 1995). Ultrasonication improves the accessibility and reactivity of the cellulose with acid (Tang *et al.* 2005). Previously, nanocellulose has been extracted from wood using high-intensity ultrasonication combined with chemical pretreatments (Chen *et al.* 2011). Many researchers have applied ultrasonication after the acid hydrolysis of cellulose for better dispersion of the NCC product (Dujardin *et al.* 2003; Beck-Candanedo *et al.* 2005). However, to the best of our knowledge, less attention has been paid to the delignification of dried stalk of *Corchorus olitorius*, usually known as jute stick powder by a microwave-assisted alkaline peroxide pulping process (AHP), thereby extracting nanocrystalline cellulose (NCC) through the ultrasound-assisted hydrolysis process.

The extraction of nano-fibrillated cellulose using an alkali pretreatment process and acid hydrolysis has been investigated extensively. Nevertheless, the industrial-scale application of concentrated acidic medium has several limitations, such as corrosion of the reaction unit, lower yield of cellulosic substrate, char formation without careful optimization of process parameters, and the recovery and recycling of acidic effluents with the successive handling of hazardous waste. Harsh conditions or an inappropriate hydrolyzing medium will result in further dissolution of the extracted cellulose to yield different types of organic compounds as a liquid fraction, rather than solid cellulosic substances (Hamid *et al.* 2014; Karim *et al.* 2014). Recently, a new type of solvent – ionic liquids (ILs) – has become extensively used for pretreatment and extraction of nanocellulose from biomass and microcrystalline cellulose due to its versatile properties (Man *et al.* 2011; Han *et al.* 2013). Ionic liquids are organic salts having an organic cation and an inorganic anion. ILs are often considered as “green solvents” as these do not form any toxic or explosive gases (Anderson *et al.* 2002). Compared to traditional solvents, they have high thermal stabilities, low melting points, and low flammability with non-volatility (Holm and Lassi 2011; Han *et al.* 2013). However, there is little information available on the effects of a combination of alkali pretreatment with chlorite-free peroxide pulping process using hydrogen peroxide (H_2O_2) for the delignification of jute stalk biomass. The crude cellulose thus obtained was hydrolyzed using acid (H_2SO_4) as well as ionic liquid ($[EMIM]^+Cl^-$) to extract nanocrystalline cellulose (NCC). The physicochemical characteristics of nanocellulose obtained after ultrasonication using different hydrolyzing mediums were studied. Field emission scanning electron microscope (FESEM) images, transmission electron microscopy (TEM), Fourier transform infrared (FT-IR) spectra, X-ray diffraction (XRD) patterns, and thermogravimetric analysis (TGA) of untreated, pretreated, bleached, and extracted nanocellulose were examined and analyzed to reveal the influence of microwave irradiation as well as ultrasonication on the structure and chemical composition of the starting biomass substrate.

EXPERIMENTAL

Materials

The starting biomass sample of dried jute stalk (S-1) was commercially available from the Bangladesh Jute Research Institute. The jute stalks (S-1) were ground and sieved. The material was passed through a 100-mesh screen to remove large particles. The average particle size of the biomass sample was kept at approximately 0.8 to 1.0 mm. The ground jute stalk powder (S-1) was dried at 110 °C for 24 h and stored in a sealed container before initial characterization. Concentrated sulfuric acid (H_2SO_4-99% purity), the ionic liquid 1-ethyl 3-methyleimidazolium chloride ($[EMIM]^+Cl^-$), sodium hydroxide (NaOH), and hydrogen peroxide (H_2O_2) were purchased from Sigma Aldrich, Malaysia. The chemicals purchased were of analytical grade.

Methods

Pretreatment of biomass

The dried biomass sample was pretreated with 2.5 M NaOH under microwave irradiation, where the biomass to solvent ratio was kept at 1:30, *i.e.* 1 g of biomass was pretreated with 30 mL of 2.5 M NaOH solution. During microwave pretreatment, the power was kept at approximately 350 W. The sample was heated for 45 min at a temperature of approximately 90 °C. The slurry thus obtained was cooled to room temperature and filtered through Whatman filter paper No. 3. The pulp thus obtained as filter cake was washed with hot deionized water several times until the filtrate reached a neutral pH. The sample was oven-dried at 60 °C and sent for characterization. The starting raw biomass (S-1) and microwave-assisted alkali pretreated sample (S-2) was characterized using scanning electron microscope (SEM) and transmission electron microscope (TEM) analyses, FTIR spectroscopy, XRD, and thermogravimetric analysis (TGA). To ensure complete delignification, the alkali-pretreated sample (S-2) was bleached using 30% H_2O_2 for 4 h at a temperature of 55 °C. The bleaching process was performed by adding 1 g of pretreated sample (S-1) with 30 mL of 30% H_2O_2 solution. The resulting sample was repeatedly washed with hot deionized water, oven-dried at 60 °C, stored in an airtight container for further characterization, and labeled as S-3.

Hydrolysis of pulp

The bleached sample (S-3) was subjected to hydrolysis using 1 M 1-ethyl 3-methyleimidazolium chloride, $[EMIM]^+Cl^-$ (S-4) and 1 M sulfuric acid, H_2SO_4 (S-5) using ultrasonication for 35 min, where the power was kept constant at 90 W at temperature 90 ^oC. At this stage, 1 g of bleached sample was (S-3) was mixed with 20 mL of hydrolyzing medium. Prepared NCC samples were freeze-dried and stored for further characterization.

Chemical composition analysis

The percentage of α-cellulose was determined by ASTM D1103-55T. The percentage of lignin and holocellulose was determined using ASTM D-1106-56 and ASTM D 1104-56. The difference between holocellulose and α-cellulose gives hemicellulose content of the sample. The moisture content was estimated using ASTM D4442-92.Triplicate tests were carried out and the average values are reported.

Morphology analysis

The changes in morphological features of acid-hydrolyzed nanocellulose (S-5) and ionic liquid-treated nanocellulose (S-4) were observed using a scanning electron microscope (SEM, Model Leo Supra 50VP Field Emission, UK). The sample after consecutive treatment of pulping and hydrolyzing along with the raw sample was placed on black carbon tape before capturing the image. The morphology of the ultrasonicated sample in the presence of different catalytic solvents was observed using an HR-TEM model JEOL JEM-2100F (Japan) field emission electron microscope with a voltage of 200 kV. The NCC samples were deposited from an aqueous dilute dispersion onto the surface of copper grids and allowed to dry in vacuum desiccator before analysis.

The changes in the chemical functional groups were verified using the infrared spectroscopy technique. FTIR spectra for the raw biomass and cellulosic samples were recorded using Bruker spectrometer model IFS 66V/S (USA). The test samples were prepared by mixing the sample with KBr at a fixed ratio to fabricate a translucent disc. The FT-IR spectra were recorded in the range of 400 to 4000 cm^{-1}.

The crystalline structure of the samples was analyzed using X-ray diffraction (XRD, Burker AXSD8 Avance, Germany) at 40 kV and 40 mA using Cu-Kα radiation sources. A continuous 2θ scan mode from 5° - 60° was applied for high degree scanning at step size of 0.02 and step time of 2s.

The percentage of crystallinity was calculated according to Eq. 1 (Terinte *et al.* 2011; Segal *et al.* 1959):

$$C = \frac{I_{002} - I_{am}}{I_{002}} \times 100 \qquad (1)$$

Here, C is the percentage of crystallinity, I_{002} is the maximum intensity of the 002 peak at $2\theta = 22.5°$, and I_{am} is the intensity at $2\theta = 18.7°$.

Thermogravimetric analysis coupled with a differential thermal analyzer (DTA) (Mettler Toledo Star SW901, Japan) was carried out to determine the thermal stability of the samples under a 10 mL/min nitrogen flow. In the TGA analysis, 5 mg of each sample was heated under a N_2 flow at 1000 °C with a heating rate of 10 °C/min.

RESULTS AND DISCUSSION

Chemical Composition analysis

The chemical composition of the sample at different stages was determined, and results are listed in Table 1. The untreated sample showed the highest proportion of hemicellulose and lignin with the lowest percentages of α-cellulose. After the microwave assisted alkali pretreatment and bleaching, the proportion of α-cellulose increased whereas hemicellulose and lignin percentages were decreased. Ultrasonication in presence of ionic liquid and acid hydrolyzing medium effectively dissolved lignin and hemicellulose from the sample. During alkali treatment α-ether linkages between lignin and hemicellulose were disrupted (Xiao *et al.* 2001). After bleaching, only a trace amount of lignin was present inside the sample.

Table 1. Chemical Composition Analysis of Untreated jute stalk (S-1), Microwave-assisted alkaline-treated jute stalk (S-2), Bleached jute stalk (S-3), $[EMIM]^+Cl^-$ treated jute stalk (S-4), and H_2SO_4 treated jute stalk (S-5)

Sample	α-cellulose (%)	Hemicellulose (%)	Lignin (%)	Moisture content (%)	Yield (%)
Untreated jute stalk S-1	64.30±1.7	17.5±1.4	6.9±0.45	11.3±0.3	-
Microwave-assisted alkaline-treated jute stalk (S-2)	76.08±1.5	11.21±0.89	1.21±0.66	11.5±0.2	68.65
Bleached jute stalk (S-3)	84.32±1.12	2.98±0.77	0.72±0.31	11.6±0.3	59.63
$[EMIM]^+Cl^-$ treated jute stalk (S-4)	87.09±1.34	0.57±0.21	0.54±0.21	11.8±0.4	48.33
H_2SO_4 treated jute stalk (S-5)	93.89±1.03	0.32±0.12	0.22±0.13	11.7±0.5	42.98

The moisture content increased slightly after the successive pretreatment process. As the cellulosic content increased after the pretreatment process, the rate of moisture adsorption also increased. There are three free –OH groups in cellulose, and these enhance the rate of moisture adsorption (Cherian *et al*. 2010). During alkali pretreatment, swelling of fiber caused development of hydrophilic ionic groups over the surface, which promoted water absorption by the bleached sample (Deepa *et al.* 2011).

The yield percentages were decreasing with successive pretreatment steps (Table 1). This phenomenon was expected, as alkaline per oxide pulping process was reducing lignin and hemicellulose content of the fiber and making the fiber more susceptible to be disrupted by hydrolyzing medium. Ultrasonication in the presence of acid and ionic liquid medium hydrolyzed the amorphous region of cellulose up to a certain extent as well as some portion of cellulosic fragments were completely broken to yield soluble oligo- and mono-saccharides.

FTIR Analysis

Cellulose fibers extracted after successive chemical treatments, along with untreated samples, were analyzed using FTIR spectroscopy to observe changes in the chemical structure of the biomass. The broad absorption peak at approximately 3394 to 3390 cm^{-1} appeared as a result of stretching of H-bonded -OH groups of the cellulose chain, whereas the band at 2900 to 2800 cm^{-1} can be ascribed to C-H stretching (Wang *et al.* 2007a; Chirayil *et al.* 2014). The most significant absorption bands observed in the FTIR spectra of all the samples near 1055 cm^{-1} can be assigned to the C–O–C stretching vibration of the pyranose ring and glycosidic ether linkages between the glucose units in cellulose, respectively (Alemdar and Sain 2008). The peak observed at 1500 to 1510 cm^{-1} for untreated biomass, alkali-treated samples, and bleached samples represents the aromatic ring vibration of lignin (Sun *et al*. 2005; Chen *et al*. 2011). However, the peak intensity decreased after alkali pretreatment and the peroxide bleaching process, reflecting the partial delignification of the sample. The peak in this region almost disappeared after the ultrasonication process using sulfuric acid and ionic liquid. The peaks observed near 1620 to 1650 cm^{-1} for all the samples can be attributed to -O-H bending vibration of adsorbed water (Mandal and Chakrabarti 2011). The band around 1069 to 1080 cm^{-1} represents C=C band vibration of aromatic ring, which was reduced after the treatment (Sun *et al.* 2005). The sharp bands ranging between 899 and 893 cm^{-1} have been attributed to the β-glycosidic linkage between the sugar units in cellulose (Sekkal *et al.* 1995).

The minor peaks appearing at around 1448, 1385, 1349, 1267, 1177, 1035, and 899 cm^{-1} are associated with the typical cellulosic bands inside the sample (Sun *et al.* 2005). During the microwave-assisted pretreatment process, the NaOH penetrates the lignocellulosic structure more efficiently. This initiates the disruption of some bands associated with lignin and hemicellulose. Basically, the alkali sodium hydroxide acts as a microwave absorber. Thus a uniform microwave heating process takes place, leading to changes in the biomass structure and composition to a greater extent. Similar observations were previously reported for the microwave-assisted alkaline pretreatment of oil palm trunk and empty fruit bunch (Lai and Idris 2013). Table 2 provides the list of major vibrational frequencies (cm^{-1}) in the FTIR spectra of the sample prepared at different stages.

Table 2. Vibrational Frequencies in FTIR Spectra of Sample at Different Stages

Sample	-OH stretching	-CH vibration	Absorbed water	C=C vibration of aromatic ring	-CH stretching	β Glycosidic Linkages
Untreated jute stalk S-1	3394	2932	1650	1502	1358	899
Microwave-assisted alkaline-treated jute stalk (S-2)	3393	2930	1643	1504	1362	897
Bleached jute stalk (S-3)	3392	2926	1639	1510	1345	895
$[EMIM]^+Cl^-$ treated jute stalk (S-4)	3391	2925	1635	-	1357	896
H_2SO_4 treated jute stalk (S-5)	3390	2910	1629	-	1364	894

SEM and TEM Analysis

The surface textural features of S-1, S-2, S-3, and S-4 samples were observed by SEM analysis and are illustrated in Fig. 1. The surface of the untreated sample was comparatively smooth because of the presence of an outer non-cellulosic layer composed of pectin, wax, lignin, and hemicellulose, which acted as cementing materials to hold the fibers in bundles (Fig. 1(a)). After microwave-assisted alkaline pretreatment of S-1, partial delignification occurred, and the surface became rough and uneven, with some folds (Fig. 1(b)).

After bleaching with H_2O_2, the fiber bundles were further separated into micro-fibrillated cellulose. Occasional pores were visible over the surface (Fig. 1(c)). During bleaching, further removal of amorphous materials (lignin, hemicellulose) from the inner matrix of the biomass substrate took place via depolymerization and defibrillation. The microfibrils were separated from each other (Abraham *et al.* 2011). Similar morphological change was previously reported for bleaching of steam exploded banana fiber (Deepa *et al.* 2015). The structure clearly reveals that successive treatment with microwave-assisted alkaline peroxide pulping process aids in hemicellulose and extractive removal with delignification of the sample. This observation was previously supported by our FTIR analysis.

Figures 1(d) and 1(e) show the surface of ultrasound-assisted $[EMIM]^+Cl^-$ and H_2SO_4 hydrolyzed samples. After hydrolysis and drying, the sample tended to be self-assembled into micro-fibrillated fiber. This is attributed to the increase of strong inter-fibrillar attraction *via* the hydrogen bonding of –OH groups of cellulose during the drying process (Jiang and Hsieh 2013 a, b). The sample surface was further eroded by hydrolysis. The dimension of the fiber was reduced because of the removal of the amorphous region of cellulose. The erosion of hydrolyzed samples (S-4 and S-5) may be caused by the emission of heat and excited species during ultrasonication. The cavitation effect of ultrasonication forms microbubbles. The high-velocity movement of these microbubbles reduces cohesion between the microfibrils (Li *et al.* 2011).

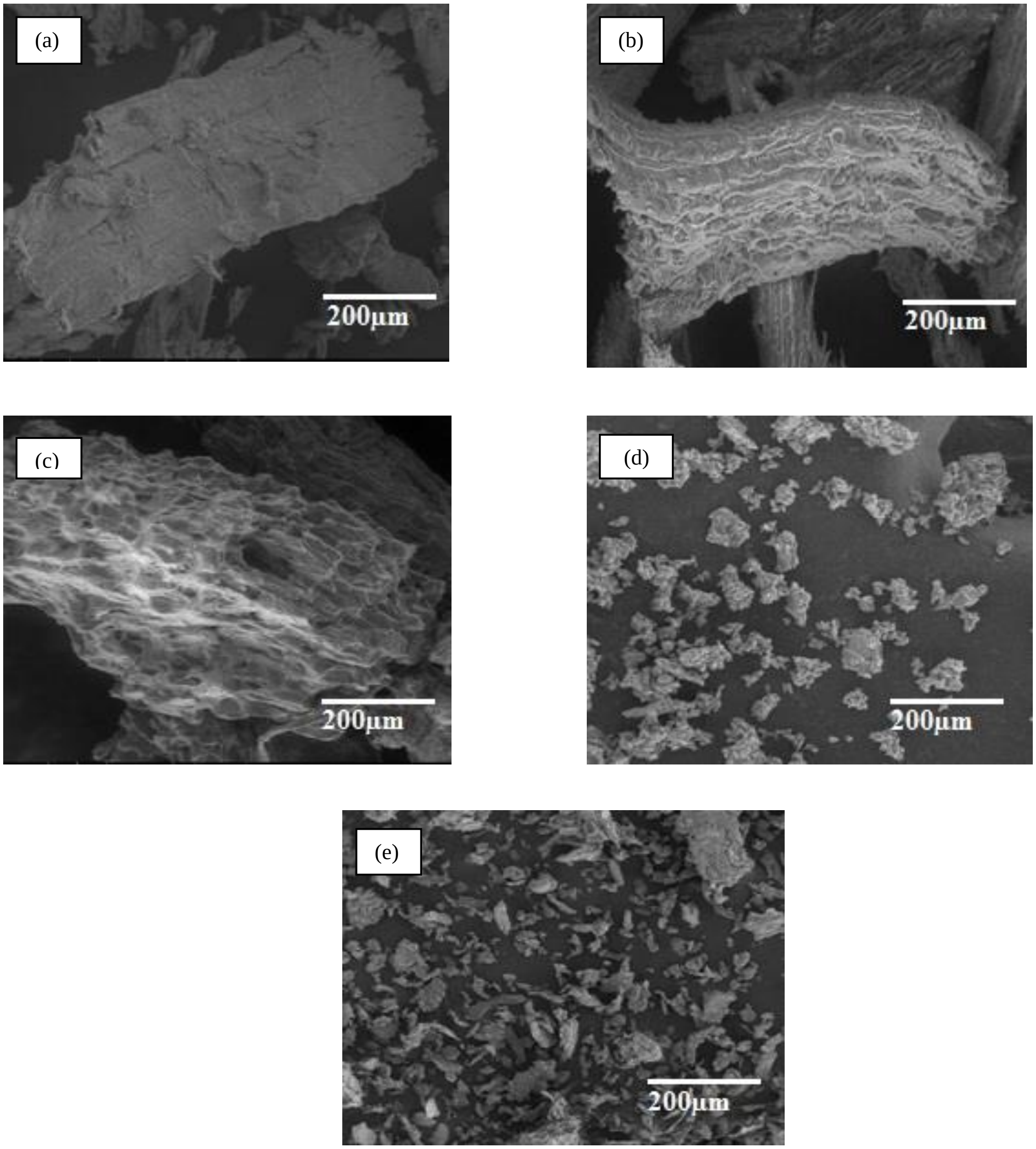

Fig. 1. SEM images of (a) untreated jute stalk (S-1); (b) microwave-assisted alkaline-treated jute stalk (S-2); (c) bleached jute stalk (S-3); (d) ionic liquid ($[EMIM]^{+}Cl^{-}$) treated jute stalk (S-4); and (e) sulfuric acid (H_2SO_4) treated jute stalk (S-5)

Transmission electron microscopy images (TEM) were acquired after ultrasonication to observe the structures of the extracted cellulose samples in the presence of different hydrolyzing media. The fibers were overlapping each other due to evaporation of water and were forming large aggregates consisting of wire like cellulosic fibers. A number of partially individualized nano-fibers were attached with the large aggregates as well (Fig. 2(a)). The crude cellulose obtained after alkaline per oxide pulping process contains highly crystalline and amorphous domain. The inter- and intra-molecular hydrogen bonds need to be broken to obtain nanocellulose. Previous literature stated that interactions between –OH groups of cellulose and anion of ionic liquids played a crucial role in this process (Han *et al*. 2013). When delignified sample (S-3) was added with $[EMIM]^+Cl^-$, the ion pairs were dissociated to give $[EMIM]^+$ cation and Cl^- anion. The hydrogen and oxygen atom of –OH groups of cellulose would form electron donor-electron acceptor complexes with the cation and anion of the ionic liquid (Pinkert *et al.* 2009). The dissociated $[EMIM]^+Cl^-$ could enter the space inside the polymeric chain of cellulose where the free Cl^- could associate with hydroxyl proton of H-O---H bonds while positive $[EMIM]^+$ could attack the oxygen of H-O--H bonds. This interaction would cause swelling of the fiber with separation of -OH groups of the different cellulose chain (Han *et al.* 2013; Holm and Lassi 2011). Inside the single cellulose chain, Cl^- ion would interact with the carbon of β-1,4 glycosidic bonds and $[EMIM]^+$ with its electron rich л system would attack oxygen atom of β-1,4 glycosidic bonds. This would disintegrate the hydrogen bonding between two cellulosic chains with disruption of β-1,4 glycosidic bonds within single cellulosic chain (Han *et al.* 2013). Thus depolymerization of crude cellulose took place to yield nanocrystalline cellulose. The cellulose fiber isolated after ultrasonication in the presence of $[EMIM]^+Cl^-$ was comparatively long and fibrillated (Fig. 2(a)). The average length was 105 nm, and the average width was 12 to 15 nm. After ultrasonication in the presence of an acid, the sample became rod-like (Fig. 2(b)). The average length of the sample was 92 nm, and the average width was 10 to 12 nm. The number of individualized cellulose nano-crystals increased after acid hydrolysis. This reveals that the ultrasound-assisted acid hydrolysis process was efficient for the scission of long chain cellulose biopolymers.

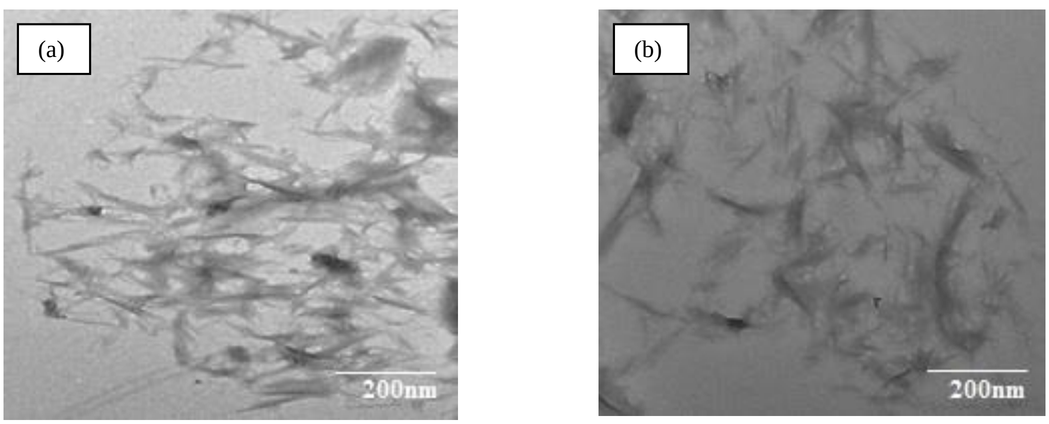

Fig. 2. TEM images of (a) Ionic liquid ($[EMIM]^+Cl^-$) treated jute stalk (S-4); and (b) sulfuric acid (H_2SO_4) treated jute stalk (S-5)

It has been reported that bonding inside the cellulose polymer can be broken by ultrasonic cavitation. This process causes solvo-dynamic shear, which involves the nucleation, growth, and collapse of micro-bubbles inside the solution (Caruso *et al.* 2009). Some bubbles in a certain size range may suddenly collapse during ultrasonication. This would create shock waves, which can generate large amounts of mechanical and thermal energy inside the solution. Thus, the hydrolyzing solution comes in contact with the cellulose surface at a velocity of several hundred meters per second. This ensures morphological changes in cellulose by enhancing its hygroscopicity. This further facilitates easy penetration of the solvent (Cintas and Luche 1999; Tang *et al.* 2005; Li and Renneckar

2009; Moon *et al*. 2011). The violent collapse induces microjets over the surface of the cellulose resulting erosion of the surface to split the fiber along the axial direction. The impact of sonication can easily break the hydrogen bond inside the fiber matrix and gradually disintegrate the micron sized cellulose fibers into nanofibers (Tischer *et al.* 2010).

XRD Analysis

XRD studies of untreated jute stalk (S-1) along with cellulosic samples after treatment (S-2, S-3, S-4, and S-5) were conducted to investigate the crystalline behavior of these fibers, and results are illustrated in Fig. 3. All the diffractograms showed two peaks at approximately $2\theta =$ 14.0° to 16.0° and 22.0° to 24.0°, which are thought to represent the typical cellulose I structure (Nishiyama *et al.* 2003). This indicated that the crystalline structure of cellulose was not completely changed during the alkaline per oxide pulping and ultrasonication treatment (Chen *et al.* 2011; Li *et al.* 2014). The peak at approximately 2θ = 14.0° to 16.0° is classified as a secondary peak for the amorphous region of cellulose, whereas the primary peak near 22.0° to 24.0° represents the crystalline region of cellulose (Liu *et al.* 2012).

The crystallinity of the sample was increased significantly when untreated jute stalk (S-1) was converted to nanocellulose (Table 3). After microwave-assisted alkali pretreatment and the bleaching process, the crystallinity index increased. The increase in the crystallinity index might be attributed to the delignification of the sample (Binod *et al.* 2012). Dissolution of the amorphous phase took place along with hemicellulose removal. Thus, the resulting nanocellulose after ultrasonication in the presence of ionic liquid and sulfuric acid (S-4 and S-5) further showed a higher crystallinity index. The untreated jute stalk had a crystallinity index of 55.36%, which after alkali pretreatment and bleaching became 63.89% and 72.44%, respectively. However, ultrasonication using H_2SO_4 treatment provided NCC samples with a higher crystallinity index (88.32%) than $[EMIM]^+Cl^-$ treated samples (83.42%) (Table 3).

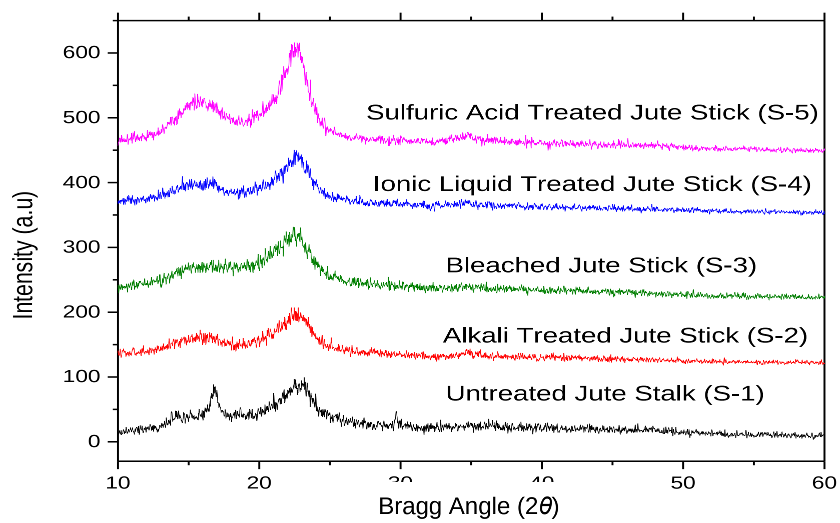

Fig. 3. XRD Diffraction of (a) untreated jute stalk (S-1); (b) microwave-assisted alkali-pretreated jute stalk (S-2); (c) bleached jute stalk (S-3); (d) ionic liquid ($[EMIM]^+Cl^-$)-hydrolyzed jute stalk (S-4); and (e) sulfuric acid (H_2SO_4) hydrolyzed jute stalk (S-5)

The extent of increase of crystallinity in chemically treated sample compared to the untreated one can be attributed to the effective elimination of lignin and hemicellulose from the amorphous region of cellulose (Li *et al.* 2014).The intensity of the secondary peak after successive pretreatment displayed a certain proportion of reduction, indicating a disruption in the amorphous region.

NaOH solution under microwave irradiation effectively acts as an intra-crystalline swelling agent, which selectively penetrates and swells the amorphous domain of cellulose (Wang *et al.* 2007b). As a result, the sample was partially delignified. After bleaching, the microfibrils were separated further. Thus, the surface area and porosity of cellulose increased, which eventually facilitated the accessibility of hydrolyzing solvent during ultrasonication. This results in disintegration of long chain polymer of cellulose to yield nano dimensional cellulose with higher crystallinity. The increase in crystallinity can increase the tensile strength and stiffness of the cellulosic fiber owing to the highly ordered, compact molecular structure among the cellulose molecules. This can further enhance Young's modulus along the longitudinal directions (Li *et al.* 2014). Thus it can be concluded that the combined application of microwave assisted alkaline per oxide pulping process with hydrolysis could be efficient to obtain nanocrystalline cellulose (NCC) which can be used as a better reinforcing agent in composite preparation.

TGA Analysis

The thermal stability of the cellulose biopolymer is a crucial aspect of its impending application as a reinforcing agent for the preparation of bionanocomposites. The thermal stability of a polymeric material is known to depend on physicochemical characteristics as well as on intermolecular interactions between the various monomer units (Maiti *et al.* 2013). The thermal stability of untreated jute stalk and extracted cellulose after two consecutive treatments was investigated using the thermogravimetric method. The thermal degradation curve for untreated samples shows several stages, indicating the presence of bio-macromolecules of lignin, hemicellulose, and cellulose that decompose at different temperatures.

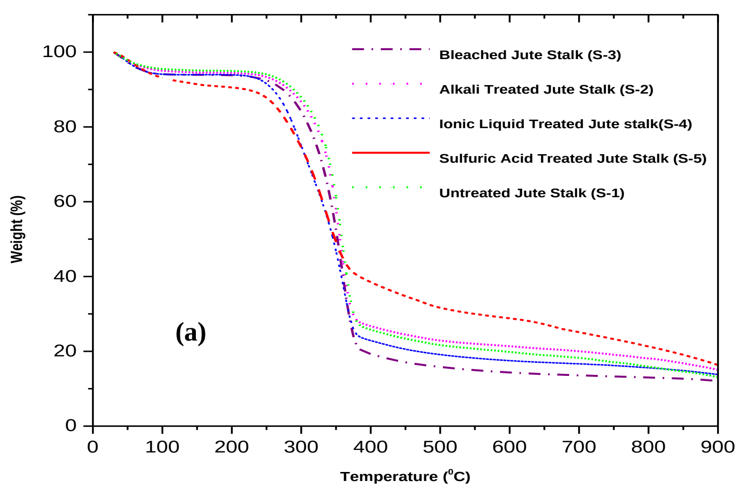

Fig. 4(a). TGA spectra for untreated jute stalk (S-1); microwave-assisted alkali-treated jute stalk (S-2); bleached jute stalk (S-3); ionic liquid ($[EMIM]^+Cl^-$) treated jute stalk (S-4); and sulfuric acid (H_2SO_4) treated jute stalk (S-5)

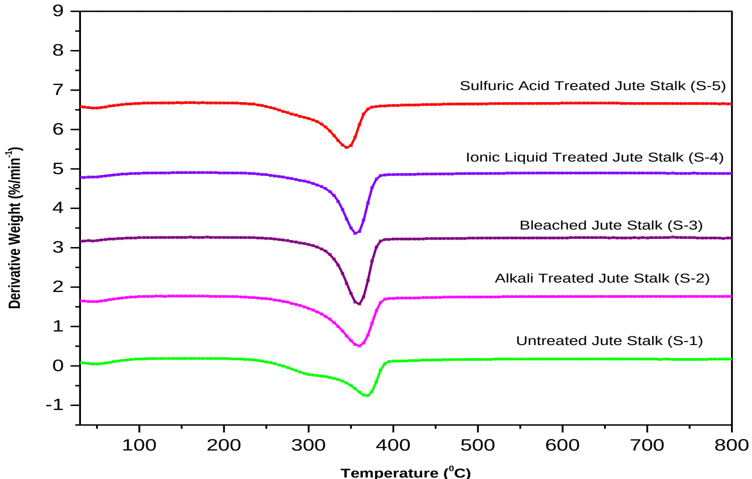

Fig. 4(b). DTG spectra for untreated jute stalk (S-1); microwave-assisted alkali-treated jute stalk (S-2); bleached jute stalk (S-3); ionic liquid ($[EMIM]^{+}Cl^{-}$) treated jute stalk (S-4); and sulfuric acid (H_2SO_4) treated jute stalk (S-5)

The first degradation step at approximately 70 to 100 °C corresponds to the evaporation of chemisorbed water (weight loss 3.2% for S-1, 2.8% for S-2, 2.6% for S-3, 1.8% for S-4, and 1.4% for S-5). The second degradation step proceeds in the temperature range of 220 to 365 °C for all the samples. This is mostly from the thermal decomposition of hemicelluloses and some portion of lignin. The major decomposition step was observed at high temperatures of approximately 300 to 400 °C, which accounts for the pyrolysis of cellulose. The cellulosic component decomposes at this temperature. However, the decomposition of lignin is far more difficult because of the presence of phenyl groups. Thus lignin decomposition takes place throughout the whole temperature range, starting below 200 °C and up to 800 °C.

In the case of untreated jute stalk (S-1), alkali-treated jute stalk (S-2), bleached jute stalk (S-3), $[EMIM]^{+}Cl^{-}$ treated samples (S-4), and H_2SO_4 treated samples (S-5), the peak temperatures corresponding to the degradation of cellulose were found to be 365, 363, 360, 358, and 353 °C, respectively. Thermal decomposition for both ionic liquid and acid-treated samples shifted to a lower temperature. This demonstrated the lower thermal stability of the extracted NCC samples resulting from the nano size of the sample and larger number of free ends of chains in the NCC sample (Li *et al.* 2011). Table 3 showed major decomposition temperature with crystallinity index and char residues for all the samples.

The char residues obtained for untreated sample was highest (16.78%). After successive treatment of alkalization and bleaching it was reduced. This is due to partial removal of lignin and hemicellulose from the biomass matrix. The amount of residues were further reduced for ionic liquid (S-4) and acid hydrolyzed sample (S-5), reflecting complete removal of lignin and hemicellulose from the starting biomass sample (S-1). Similar phenomenon was previously reported for preparation of nano cellulose from de-pectinated sugar beet pulp (Li *et al.* 2014) and sisal fiber (Deepa *et al.* 2015).

Table 3. Degradation Characteristics and Char Residues at Different Stages of Treatment

Sample	DTG_{max} (°C)	Char Residues (%)	Crystallinity Index (%)
Untreated jute stalk (S-1)	365	16.78	55.36
Microwave-assisted alkaline-treated jute stalk (S-2)	363	13.66	63.89
Bleached jute stalk (S-3)	360	12.78	72.44
$[EMIM]^+Cl^-$ treated jute stalk (S-4)	353	11.39	83.42
H_2SO_4 treated jute stalk (S-5)	358	11.99	88.32

CONCLUSIONS

1. Nanocrystalline cellulose (NCC) with a high crystallinity index was successfully synthesized from dried jute stalk (S-1) using a novel method that combined a microwave-assisted pretreatment method with ultrasonication in the presence of various hydrolyzing mediums. The crystallinity index reached up to 88.32% and 83.42%, respectively for H_2SO_4 and $[EMIM]^+ Cl^-$ hydrolysis process.
2. Microwave-assisted alkali pretreatment caused the partial delignification of jute stalk samples. A chlorite-free bleaching process using H_2O_2 further removed a substantial amount of lignin and the surface of the sample was eroded, leading to defibrillation. This provided more active sites for the penetration of the hydrolyzing medium during ultrasonication.
3. Thermogravimetric analysis of the NCC sample showed lower thermal stability compared with untreated jute stalk, alkali-treated samples, and bleached samples. This was caused by the smaller size and higher number of free ends of macromolecular chains of the cellulosic sample.
4. Alone, a microwave-assisted alkali pretreatment process and bleaching using H_2O_2 was not sufficient enough for the complete removal of lignin. Further ultrasonication in the presence of acid and ionic liquid was required to extract NCC samples with a higher crystallinity index.
5. In this research, a green and sustainable approach of using $[EMIM]^+ Cl^-$ with traditional H_2SO_4 acid hydrolysis was compared to extract NCC sample from jute stalk. The yield percentage obtained using $[EMIM]^+ Cl^-$ hydrolysis (48.33%) process was higher than the H_2SO_4 hydrolysis (42.98%) process.

ACKNOWLEDGMENTS

The authors would like to thank BKP (BK054-2015) and High Impact Research (HIR F-000032) of University Malaya, Malaysia for their cordial support in completing this work.

REFERENCES CITED

Abdul Khalil, H. P. S., Davoudpour, Y., Islam, M. N., Mustapha, A., Sudesh, K., Dungani, R., and Jawaid, M. (2014). "Production and modification of nanofibrillated cellulose using various mechanical processes: A review," *Carbohydr. Polym.* 99, 649-665. DOI: 10.1016/j.carbpol.2013.08.069

Abraham, E., Deepa, B., Pothan, L. A., Jacob, M., Thomas, S., Cvelbar, U., and Anand, R. (2011). "Extraction of nanocellulose fibrils from lignocellulosic fibres: A novel approach," *Carbohydr Polym*, 86 (4) 1468-1475. DOI.10.1016/j.carbpol.2011.06.034.

Alemdar, A., and Sain, M. (2008). "Isolation and characterization of nanofibers from agricultural residues—Wheat straw and soy hulls," *Bioresour. Technol.* 99, 1664-1671. DOI: 10.1016/j.biortech.2007.04.029

Anderson, J. L., Ding, J., Welton, T., and Armstrong, D. W. (2002). "Characterizing ionic liquids on the basis of multiple salvation interactions," *J. Am. Chem. Soc.* 124 (47), 14253-14254. DOI: 10.1021/ja028156h.

Araki, J., and Kuga, S. (2001). "Effect of trace electrolytes on liquid crystal type of cellulose microcrystals," *Langmuir* 17(15), 4493-4496. DOI: 10.1021/la0102455.

Beck-Candanedo, S., Roman, M., and Gray, D. G. (2005). "Effect of reaction conditions on the properties and behavior of wood cellulose nanocrystal suspensions," *Biomacromolecules* 6(2), 1048-1054. DOI: 10.1021/bm049300p

Binod, P., Satyanagalakshmi, K., Sindhu, R., Janu, K. U., Sukumaran, R. K., and Pandey, A. (2012). "Short duration microwave assisted pretreatment enhances the enzymatic saccharification and fermentable sugar yield from sugarcane bagasse," *Renew. Energ.* 37(1), 109-116. DOI: 10.1016/j.renene.2011.06.007

Chakraborty, A., Sain, M., and Kortschot, M. (2005). "Cellulose micro-fibrils: A novel method of preparation using high shear refining and cryocrushing," *Holzforschung* 59, 102-107. DOI: 10.1515/HF.2005.016

Chen, W. S., Yu, H. P., Liu, Y. X., Chen, P., Zhang, M. X., and Hai, Y. F. (2011). "Individualization of cellulose nanofibers from wood using high-intensity ultrasonication combined with chemical pretreatments," *Carbohydr. Polym.* 83(4), 1804-1811. DOI: 10.1016/j.carbpol.2010.10.040

Cherian, B. M., Leão, A.L., De Souza, S. F., Thomas, S., Pothan, L. A., and Kottaisamy, M. (2010). "Isolation of nanocellulose from pineapple leaf fibres by steam explosion," *Carbohydr. Polym.* 81 (3), 720–725. DOI: 10.1016/j.carbpol.2010.03.046.

Chirayil, C. J., Joy, J., Mathew, L., Mozetic, M., Koetz, J., and Thomas, S. (2014). "Isolation and characterization of cellulose nanofibrils from *Helicteres isora* plant," *Ind. Crop Prod.* 59, 27-34. DOI: 10.1016/j.indcrop.2014.04.020

Caruso, M. M., Davis, D. A., Shen, Q. L., Odom, S. A., Sottos, N. R., White, S. R., and Moore, J. S. (2009). "Mechanically-induced chemical changes in polymeric materials," *Chem. Rev.* 109(11), 5755-5798. DOI: 10.1021/cr9001353

Cintas, P., and Luche, J. L. (1999). "Green chemistry: The sonochemical approach," *Green Chem.* 1(3), 115-125. DOI: 10.1039/A900593E

Chowdhury, Z. Z., Zain, S. M., Hamid, S. B. A., and Khalid, K. (2014). "Catalytic role of ionic liquids for dissolution and degradation of biomacromolecules," *BioResources* 9(1), 1787-1823. DOI: 10.15376/biores.9.1.1787-1823

Das, K., Ray, D., Bandyopadhyay, N. R., Sahoo, S., Mohanty, A. K., and Misra, M. (2011). "Physicomechanical properties of the jute micro/nanofibril reinforced starch/polyvinyl alcohol bio-composite films," *Compos. Part B* 42(3), 376-381. DOI: 10.1016/j.compositesb.2010.12.017

Deng, H., Zhou, X., Wang, X., Zhang, C., Ding, B., Zhang, Q., and Du, Y. (2010). "Layer-by layer structured polysaccharides film coated cellulose nanofibrous mats for cell culture," *Carbohydr. Polym.* 80(2), 475-480. DOI: 10.1016/j.carbpol.2009.12.004

Deepa, B., Eldho, A., Nereida, C., Miran, M., Mathew, A. P., Oksman, K., Faria, M., Thomas, S., and Pothan, L. A. (2015). "Utilization of various lignocellulosic biomass for the production of nanocellulose: A comparative study," *Cellulose* 22, 1075-1090. DOI: 10.1007/s10570-015-0554-x.

Deepa, B. Eldho, A., Cherian, B. M., Bismarck, A., Blaker, J. J., Pothan, L. A., Leao, A. L., De Souza, S. F., and Kottaisamy, M. (2011). "Structure, morphology and characteristics of banana nanofibers obtained by steam explosion," *Bioresour. Technol.* 102(2), 1988-1997. DOI:10.1016/j.biortech.2010.09.030.

Dujardin, E., Blaseby, M., and Mann, S. (2003). "Synthesis of mesoporous silica by sol-gel mineralisation of cellulose nanorod nematic suspensions," *J. Mater. Chem.* 13(4), 696-699. DOI: 10.1039/B212689C

Favier, V., Chanzy, H., and Cavaille, J. Y. (1995). "Polymer nanocomposites reinforced by cellulose whiskers," *Macromolecules* 28(18), 6365-6367. DOI: 10.1021/ma00122a053

Ferrer, A., Filpponen, I., Rodríguez, A., Laine, J., and Rojas, O. J. (2012). "Valorization of residual empty palm fruit bunch fibers (EPFBF) by microfluidization: Production of nanofibrillated cellulose and EPFBF nanopaper," *Bioresour. Technol.* 125, 249-255. DOI: 10.1016/j.biortech.2012.08.108

Fukuzumi, H., Saito, T., and Isogai, A. (2013). "Influence of TEMPO- oxidized cellulose nanofibril length on film properties," *Carbohydr. Polym.* 93,172-177. DOI: 10.1016/j.carbpol.2012.04.069

Hamid, S. B. A., Chowdhury, Z. Z., and Karim, M. Z. (2014). "Catalytic extraction of microcrystalline cellulose (MCC) from *Elaeis guineensis* using central composite design (CCD)," *BioResources* 9(4), 7403-7426. DOI: 10.15376/biores.9.4.7403-7426

Han, J., Zhou, C., French, A. D., Han, G., and Wu, Q. (2013). "Characterization of cellulose II nanoparticles regenerated from 1-butyl-3-methylimidazolium chloride," *Carbohydr. Polym.* 94(2),773-781. DOI:10.1016/j.carbpol.2013.02.003.

Henriksson, M., and Berglund, L. A. (2007). "Structure and properties of cellulose nanocomposite films containing melamine formaldehyde," *J. Appl. Polym. Sci.* 106(4), 2817-2824. DOI: 10.1002/app.26946

Hossain, K. M. Z., Hasan, M. S., Boyd, D., Rudd, C. D., Ahmed, I., and Thielemans, W. (2014). "Effect of cellulose nanowhiskers on surface morphology, mechanical properties, and cell adhesion of melt-drawn polylactic acid fibers," *Biomacromolecules* 15(4), 1498-1506. DOI: 10.1021/bm5001444

Helbert, W., Cavaille, J. Y., and Dufresne, A. (1996). "Thermoplastic nanocomposites filled with wheat straw cellulose whiskers. Part I: Processing and mechanical behavior," *Polym. Compos.* 17(4), 604-611. DOI: 10.1002/pc.10650

Holm, J., and Lassi, U. (2011). "Ionic liquids in the pretreatment of lignocellulosic biomass," in: *Ionic Liquids: Applications and Perspectives,* pp. 545-560, ISBN: 978-953-307-248-7, In Tech Publisher, Europe. http://www.intechopen.com/books/ionic-liquids-applications-and-perspectives/ionic-liquids-in-thepretreatment-of lignocellulosic-biomass.

Iwamoto, S., Nakagaito, A. N., and Yano, H. (2007). “Nano-fibrillation of pulp fibers for the processing of transparent nanocomposites,” *Appl. Phys. A Mater.* 89(2), 461-466. DOI: 10.1007/s00339-007-4175-6

Jiang, F., and Hsieh, Y. L. (2013a). "Chemically and mechanically isolated nanocellulose and their self-assembled structures," *Carbohydr. Polym.* 95(1), 32-40. DOI: 10.1016/j.carbpol.2013.02.022

Jiang, F., Han, S., Hsieh, Y. L. (2013b). “Controlled defibrillation of rice straw cellulose and self-assembly of cellulose nanofibrils into highly crystalline fibrous materials,” *RSC Adv.* 3(30), 12366-12375. DOI: 10.1039/C3RA41646A

Kalia, S., Boufi, S., Celli, A., and Kango, S. (2014). “Nanofibrillated cellulose: Surface modification and potential applications,” *Colloid Polym. Sci.* 292(1), 5-31. DOI: 10.1007/s00396-013-3112-9

Kappe, C. O. (2009). *Practical Microwave Synthesis for Organic Chemists: Strategies, Instruments and Protocols*, Wiley, New York.

Karim, M. Z., Chowdhury, Z. Z., Hamid, S. B. A., and Ali, M. E. (2014). "Statistical optimization for acid hydrolysis of microcrystalline cellulose and its physiochemical characterization by using metal ion catalyst," *Materials* 7(10), 6982-6999. DOI: 10.3390/ma7106982.

Kengkhetkit, N., and Amornsakchai, T. (2014). “A new approach to ‘greening’ plastic composites using pineapple leaf waste for performance and cost effectiveness,” *Mater. Des.* 55, 292-299. DOI: 10.1016/j.matdes.2013.10.005.

Klemm, D., Heublein, B., Fink, H. -P., and Bohn, A. (2005). "Cellulose: Fascinating biopolymer and sustainable raw material," *Angew. Chem. Int. Ed.* 44(22), 3358-3393. DOI: 10.1002/anie.200460587

Kos, T., Alojz Anžlovar, A., Kunaver, M., Huskic, M., and Žagar, E. (2014). “Fast preparation of nanocrystalline cellulose by microwave-assisted hydrolysis,” *Cellulose*, 21, 2579-2585, DOI 10.1007/s10570-014-0315-2.

Lai, L., and Idris, A. (2013). “Disruption of oil palm trunks and fronds by microwave-alkali pretreatment,” *BioResources* 8(2), 2792-2804. DOI: 10.15376/biores.8.2.2792-2804

Li, Q. Q., and Renneckar, S. (2009). “Molecularly thin nanoparticles from cellulose: Isolation of sub-microfibrillar structures,” *Cellulose* 16(6), 1025-1032. DOI: 10.1007/s10570-009-9329-6

Li, R., Fei, J., Cai, Y., Li, Y., Feng, J., and Yao, J. (2009). "Cellulose whiskers extracted from mulberry: A novel biomass production," *Carbohydr. Polym.* 76(1), 94-99. DOI: 10.1016/j.carbpol.2008.09.034

Li, W., Wang, R., and Liu, S. (2011). “Nanocrystalline cellulose prepared from softwood kraft pulp *via* ultrasonic assisted acid hydrolysis,” *BioResources* 6(4), 4271-4281. DOI: 10.15376/biores.6.4.4271-4281

Li, J., Wei, X., Wang, Q., Chen, J., Chang, G., Kong, L., Su, J., and Liu, Y. (2012). "Homogeneous isolation of nanocellulose from sugarcane bagasse by high pressure homogenization," *Carbohydr. Polym.* 90(4), 1609-1613. DOI: 10.1016/j.carbpol.2012.07.038.

Li, M., Wang, L., Li, D., Cheng, Y., Adhikari, B. (2014). “Preparation and characterization of cellulose nanofibers from de-pectinated sugar beet pulp,” *Carbohydr. Polym*. 102(1), 136-143. DOI: 10.1016/j.carbpol.2013.11.021.

Liu, J. G., Wang, Q. H., Wang, S., Zou, D. X., and Sonomoto, K. (2012). “Utilization of microwave-NaOH pretreatment technology to improve performance and L-lactic acid yield from vinasse," *Biosyst. Eng.* 112, 6-13. DOI: 10.1016/j.biosystemseng.2012.01.004

Man, Z., Muhammad, N., Sarwono, A., Bustam, M. A., Kumar, M. V., and Rafiq, S. (2011). "Preparation of cellulose nanocrystals using an ionic liquid," *J. Polym. Environ*. 19(3), 726-31.DOI: 10.1007/s10924-011-0323-3.

Mandal, A., and Chakrabarty, D. (2011). "Isolation of nanocellulose from waste sugarcane bagasse (SCB) and its characterization," *Carbohydr. Polym.* 86(3), 1291-1299. DOI: 10.1016/j.carbpol.2011.06.030

Maiti, S., Jayaramudu, J., Das, K., Reddy, S. M., Sadiku, R., Ray, S. S., Liu, D. (2013). "Preparation and characterization of nano-cellulose with new shape from different precursor," *Carbohydr. Polym.* 98(1), 562-567. DOI: 10.1016/j.carbpol.2013.06.029

Moran, J. I., Alvarez, V. A., Cyras, V. P., and Vazquez, A. (2008). "Extraction of cellulose and preparation of nanocellulose from sisal fibers," *Cellulose* 15(1), 149-159. DOI: 10.1007/s10570-007-9145-9

Mondragon, G., Fernandes, S., Retegi, A., Peña, C., Algar, I., Eceiza, A., and Arbelaiz, A. (2014). "A common strategy to extracting cellulose nanoentities from different plants," *Ind. Crops Prod.* 55, 140-148. DOI: 10.1016/j.indcrop.2014.02.014

Morais, J. P. S., Rosa, M. de F., de Souza Filho M de Sa M., Nascimento, L. D., do Nascimento, D. M., and Cassales, A. R. (2013). "Extraction and characterization of nanocellulose structures from raw cotton linter," *Carbohydr. Polym.* 91(1), 229-235. DOI: 10.1016/j.carbpol.2012.08.010

Moon, R. J., Martini, A., Nairn, J., Simonsen, J., and Youngblood, J. (2011). "Cellulose nanomaterials review: Structure, properties and nanocomposites," *Chem. Soc. Rev.* 40(7), 3941-3994. DOI: 10.1039/C0CS00108B

Nguyen, H. D., Mai, T. T. T., Nguyen, N. B., Dang, T. D., Le, M. L. P., Dang, T. T., and Tran, V. M. (2013). "A novel method for preparing microfibrillated cellulose from bamboo fibers," *Adv. Nat. Sci.: Nanosci. Nanotechnol.* 4(1), 15-16. DOI: 10.1088/2043-6262/4/1/015016

Nakagaito, A. N., and Yano, H. (2004). "The effect of morphological changes from pulp fiber towards nano-scale fibrillated cellulose on the mechanical properties of high strength plant fiber based composites," *Appl. Phys. A Mater.* 78(4), 547-552. DOI: 10.1007/s00339-003-2453-5

Nishiyama, Y., Sugiyama, J., Chanzy, H., and Langan, P. (2003). "Crystal structure and hydrogen bonding system in cellulose Iα from synchrotron X-ray and neutron fiber diffraction," *J. Am. Chem. Soc.* 125(47), 14300-14306. DOI: 10.1021/ja037055w

Pinkert, A., Marsh, K. N., Pang, S. S., and Staiger, M. P. (2009). "Ionic liquids and their interaction with cellulose," *Chem. Rev*. 109(12), 6712-6728. DOI: 10.1021/cr9001947.

Revol, J. F., Bradford, H., Giasson, J., Marchessault, R. H., and Gray, D. G. (1992). "Helicoidal self-ordering of cellulose microfibrils in aqueous suspension," *Int. J. Biol. Macromol.* 14(3), 170-172. DOI: 10.1016/S0141-8130(05)80008-X

Roman, M., and Winter, W. T. (2004). "Effect of sulfate groups from sulfuric acid hydrolysis on the thermal degradation behavior of bacterial cellulose," *Biomacromolecules* 5(5), 1671-1677. DOI: 10.1021/bm034519+

Sekkal, M., Dincq, V., Legrand, P., and Huvenne, J. P. (1995). "Investigation of the glycosidic linkages in several oligosaccharide using FT-IR and FT-Raman spectroscopies," *J. Mol. Struct.* 349, 349-352. DOI: 10.1016/0022-2860(95)08781-P

Sheltami, R. M., Abdullah, I., Ahmad, I., Dufresne, A., and Kargarzadeh, H. (2012). "Extraction of cellulose nanocrystals from mengkuang leaves (*Pandanus tectorius*)," *Carbohydr. Polym.* 88(2), 772-779. DOI: 10.1016/j.carbpol.2012.01.062.
Silvério, H. A., Flauzino Neto, W. P. F., Dantas, N. O., and Pasquini, D. (2013). "Extraction and characterization of cellulose nanocrystals from corncob for application as reinforcing agent in nanocomposites," *Ind. Crops Prod.* 44, 427-436. DOI: 10.1016/j.indcrop.2012.10.014
Sacui, I. A., Nieuwendaal, R. C., Burnett, D. J., Stranick, S. J, Jorfi, M., Wader, C., Foster, E. J., Olsson, R. T., and Gilman, J. W. (2014). "Comparison of the properties of cellulose nanocrystals and cellulose nanofibrils isolated from bacteria, tunicate, and wood processed using acid, enzymatic, mechanical, and oxidative methods," *ACS Appl. Mater. Interfaces* 6(9), 6127-6138. DOI: 10.1021/am500359f
Stenstad, P., Andresen, M., Tanem, B. S., and Stenius, P. (2008). "Chemical surface modifications of microfibrillated cellulose," *Cellulose* 15(1), 35-45. DOI: 10.1007/s10570-007-9143-y
Segal, L., Creely, J., Martin, A., and Conrad, C. (1959). "An empirical method for estimating the degree of crystallinity of native cellulose using the X-ray diffractometer," *Textile Research Journal* 29(10), 786-794. DOI: 10.1177/004051755902901003
Sun, X. F., Xu, F., Sun, R. C., Fowler, P., and Baird, M.S. (2005). "Characterization of degraded cellulose obtained from steam exploded wheat straw," *Carbohydr. Res.* 340(1), 97-106. DOI:10.1016/j.carres.2004.10.022
Terinte, N., Ibbett, R., and Schuster, K. C. (2011). "Overview on native cellulose and microcrystalline cellulose I structure studied by X-ray diffraction (WAXD): Comparison between measurement techniques," *Lenzinger Berichte* 89, 118-131.
Tang, A. M., Zhang, H. W., Chen, G., Xie, G. H., and Liang, W. Z. (2005). "Influence of ultrasound treatment on accessibility and regioselective oxidation reactivity of cellulose," *Ultrason. Sonochem.* 12(6), 467-472. DOI: 10.1016/j.ultsonch.2004.07.003
Tischer, P. C. S. F., Sierakowski, M. R., Westfahl, H., and Tischer, C. A. (2010). "Nanostructural reorganization of bacterial cellulose by ultrasonic treatments," *Biomacromolecules* 11(5), 1217-1224. DOI: 10.1021/bm901383a.
Uma Maheswari, C., Obi Reddy, K., Edison, M., Guduri, B. R., and Rajulu, A. V. (2012). "Extraction and characterization of cellulose microfibrils from agricultural residue - *Cocos nucifera* L.," *Biomass Bioenerg.* 46, 555-563. DOI: 10.1016/j.biombioe.2012.06.039
Wang, N., Ding, E. Y., and Cheng, R. S. (2007a). "Thermal degradation behaviors of spherical cellulose nanocrystals with sulfate groups," *Polymer* 48(12), 3486-3493. DOI: 10.1016/j.polymer.2007.03.062
Wang, S. J., Yu, J. L., Yu, J. G., Chen, H. X., and Pang, J. P. (2007b). "The effect of acid hydrolysis on morphological and crystalline properties of *Rhizoma dioscorea* starch," *Food Hydrocolloids* 21(7), 1217-1222. DOI: 10.1016/j.foodhyd.2006.08.002
Wicklein, B., and Salazar-Alvarez, G. (2013). "Functional hybrids based on biogenic nanofibrils and inorganic nanomaterials," *J. Mater. Chem. A* 1(18), 5469-5478. DOI: 10.1039/C3TA01690K
Xiao, B., Sun, X. F., and Sun, R. C. (2001). "Chemical, structural, and thermal characterizations of alkali-soluble lignins and hemicelluloses, and cellulose from

maize stems, rye straw, and rice straw," *Polym. Degrad. Stab*. 74(2), 307-319. DOI: 10.1016/j.biortech.2010.09.030.
Xu, X., Liu, F., Jiang, L., Zhu, J. Y., Haagenson, D., and Wiesenborn, D. P. (2013). "Cellulose nanocrystals *vs.* cellulose nanofibrils: A comparative study on their microstructures and effects as polymer reinforcing agents," *ACS Appl. Mater. Interfaces* 5(8), 2999-3009. DOI: 10.1021/am302624t
Yin, C. (2012). "Review: Microwave-assisted pyrolysis of biomass for liquid biofuels production," *Bioresour. Technol.* 120, 273-284. DOI: 10.1016/j.biortech.2012.06.016
Zhang, Z. H., and Zhao, Z. B. K. (2010). "Microwave-assisted conversion of lignocellulosic biomass into furans in ionic liquid," *Bioresour. Technol.* 101(3), 1111-1114. DOI: 10.1016/j.biortech.2009.09.010

Article submitted: June 4, 2015; Peer review completed: July 30, 2015; Revised version received and accepted; November 21, 2015; Published: February 18, 2016.
DOI: 10.15376/biores.11.2.3397-3415